ARROW

ATMOSPHERIC INFRASOUND BY OCEAN WAVES

PRODUCT USER MANUAL

customer	IFREMER/CEA
document reference	Product User Manual
visibility	Internet
Version/Rev	1.4
Date of issue	05/02/2024

Document evolution sheet

Ed.	Rev.	Date	Purpose evolution	Authors
1	0	07/12/2021	Creation of document	M. Accensi
1	1	06/01/2022	Redaction	M. De Carlo
1	2	07/01/2022	Review	M. Accensi
1	3	04/01/2024	Public version	M. Accensi
1	4	05/02/2024	Review	A. Le Pichon P. Letournel

Contents

List of Figures

List of Tables

1 Introduction

1.1 Context

The LOPS joint research unit is a multidisciplinary laboratory with unique skills and resources in France in numerical modeling, analysis and satellite data. In particular, LOPS is at the forefront of research on directional wave spectra modeling and has developed an expertise internationally recognized for the characterization of sources of acoustic noise associated with waves, with first applications to seismology. Although having no vocation operational, Ifremer carries out daily simulations of waves all over the globe, using the state-of-the-art parameterizations of the WAVEWATCH-III (r) wave model. The simulations are performed automatically twice a day and model release time steps are currently 3 hours. To achieve these simulations, the LOPS has at its disposal the HPC DATARMOR calculation center of IFREMER (11088 cores - 426 Tflops) dedicated to intensive computation and big data hosting.

Due to their common interest in the field of the dynamics of seismic / infrasound coupling, IFREMER and the CEA worked together in the context of the thesis of Marine De Carlo, supervised by Fabrice Ardhuin (CNRS) and Alexis Le Pichon (CEA), and defended in December 2020, on the characterization of oceanic noise on a global scale from seismic-acoustic observations. In the framework of this thesis, a new theoretical description of the mechanism signal generation connecting the amplitude of the pressure signal to the height and frequency wave oscillation has been proposed.

As part of its surveillance missions, the CEA routinely uses data from the International Monitoring System (IMS), set up for the control of the Comprehensive nuclear Test Ban Treaty (CTBT). From an operational point of view, the CEA aims at improving its detection of infrasound sources, that is to say to better locate and characterize the sources of acoustic signal of interest (nuclear explosions, meteorites ...). In the frequency band of interest for monitoring nuclear explosions, oceanic generated infrasound (microbaroms) are a dominant and permanent source of noise. Better characterization of this coherent noise is expected to limit the number of false alarms and thus improve the detection capabilities of the IMS.

A systematic exploitation of the model of De Carlo et al. 2020 will allow continuous characterization sources of coherent oceanic noise to support the analysis of signals of interest drowned in this noise.

Currently, in the wave model, directional spectra are calculated but not saved entirely for reasons of storage; only the moments of the wave spectra are kept as outputs of the model. Even though these moments are sufficient for the majority of wave-related studies, they do not allow to get the sources of microbaroms. Indeed, microbaroms are generated by 2nd order nonlinear interactions between opposite waves of the same frequency. These interactions are represented by a quantity called the microseism source term, based on the Hasselmann

integral which is the integral over all directions of the product of the energy present in one direction and its opposite, at a given frequency. Therefore, to obtain the sources of microbaroms, directional spectra are necessary and the calculation of the Hasselmann integral must be carried out and kept during the construction of the model.

The graphic below shows a global vision of the data production steps, starting from the wave model output to achieve to an acoustic field at a given station.

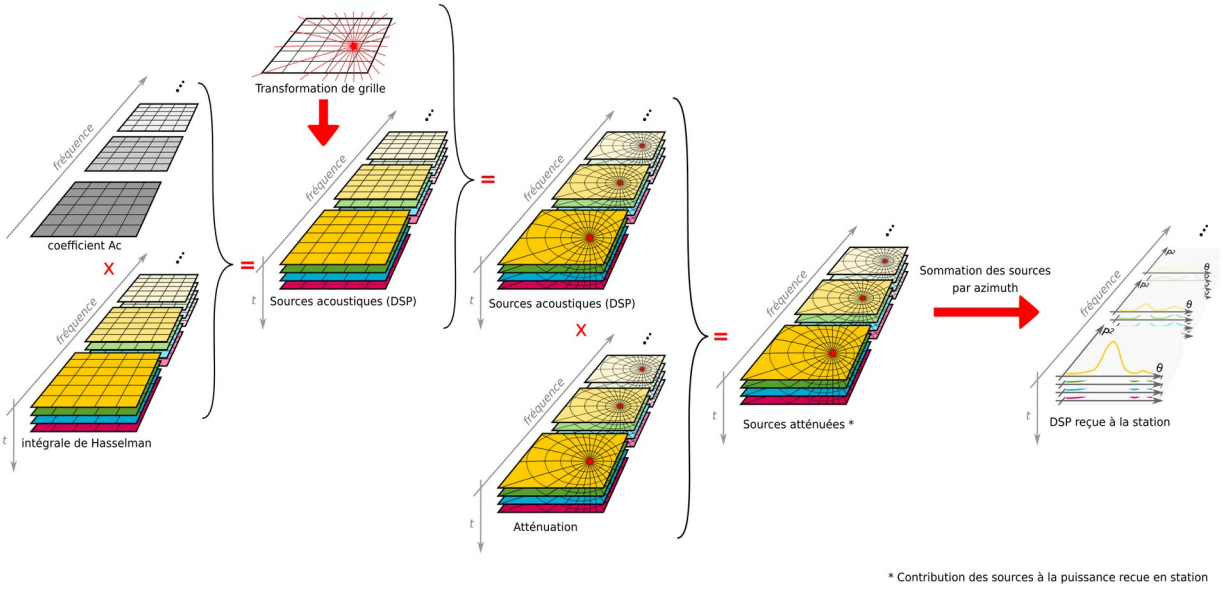

Figure 1: Descriptive graphic of the data production steps

1.2 Purpose of the document

The present document is the technical report dedicated to the description of the acoustic sources obtained from the microseism source term at the sea surface which is produced by the spectral wave model WAVEWATCH-III®.

It provides an overview of products content, format and validation.

The data production framework (methodology, algorithm, ...) is also detailed, from the worldwide production of the wave data to the acoustic field at a ground station (input/output, dependencies with external data, interfaces for visualization, hindcast and real-time production)

Finally, some considerations are addressed about data processing and usage.

1.3 Document structure

In addition to this introduction, this document includes the following chapters:

- Chapter 2 describes the product content, format and validation.
- Chapter 3 describes the data production framework.

1.4 Applicable & Reference documents

- De Carlo, M., F. Ardhuin, A. Le Pichon (2019), Atmospheric infrasound radiation from ocean waves in finite depth: a unified generation theory and application to radiation patterns, Geophys. J. Int., 221, 569–585, https://doi.org/10.1093/gji/ggaa015
- Vorobeva, E., De Carlo, M., Le Pichon, A., Espy, P. J., and Näsholm, S. P (2020), Microbarom radiation and propagation model assessment using infrasound recordings: a vespagram-based approach, Ann. Geophys. Discuss, https://doi.org/10.5194/angeo-2020-78
- De Carlo, M., Hupe, P., Le Pichon, A., Ceranna, L., and F. Ardhuin (2021), Global microbarom patterns: A first confirmation of the theory for source and propagation, Geophys. Res. Lett., 48, https://doi.org/10.1029/2020GL090163
- Waxler, R., and K. Gilbert (2007), The radiation of atmospheric microbaroms by ocean waves, J. Acoustic. Soc. Am., 119, https://doi.org/10.1121/1.2191607
- Šindelářová, T.et al. (2021), Infrasound signature of the post-tropical storm Ophelia at the Central and Eastern European Infrasound Network, J. Atmos. Solar-Terr. Phys., https://doi.org/10.1016/j.jastp.2021.105603.
- Smirnov, A. et al. 2021, Characterizing the global ocean ambient noise as recorded by the dense seismo-acoustic Kazakh network, Solid Earth, 12, 503-520, https://doi.org/10.5194/se-12-503-202.
- Alday Matias, Accensi Mickael, Ardhuin Fabrice, Dodet Guillaume (2021). A global wave parameter database for geophysical applications. Part 3: Improved forcing and spectral resolution. Ocean Modelling, 166, 101848 (19p.). https://doi.org/10.1016/j.ocemod.2021.101848
- Tolman, Hendrik & Abdolali, Ali & Mickael, Accensi & Alves, Jose-Henrique & Ardhuin, Fabrice & Babanin, Alexander & Barbariol, Francesco & Benetazzo, Alvise & Bidlot, Jean & Booij, Nico & Boutin, Guillaume & Bunney, Chris & Campbell, Tim & Chalikov, Dmitry & Chawla, Arun & Cheng, Sukun & Collins, Clarence & Filipot, Jean-François & Flampouris, Stylianos & Liang, Zhi. (2019). User manual and system documentation of WAVEWATCH III (R) version 6.07.

1.5 Terminology

CEA	Commissariat à l'Energie Atomique et aux Energies Alternatives
IFREMER	Institut Français de Recherche pour l'Exploitation de la Mer
WW3	WAVEWATCH-III®
P2L	spectral density of equivalent surface pressure
CDIP	Coastal Data Information Program
IFS	Integrated Forecast System
ECMWF	European Centre for Medium-Range Weather Forecasts
NCEP	National Centers for Environmental Prediction
INSTAC	In Situ Thematic Centre
DATARMOR	Ifremer's High Performance Computing facilities
IMS	International Monitoring System
CTBT	Comprehensive nuclear Test Ban Treaty

1.6 How to cite

1.6.1 WAVEWATCH-III (r) products

Restrictions and citations will vary depending on the data and its date of production. All data generated by WAVEWATCH-III (r) are free of use, the only requirement is to cite the following DOI :

Accensi Mickael (2020). GLOBMULTI_ERA5_GLOBCUR_01. IFREMER.

https://doi.org/10.12770/857a3337-f59a-481a-bf98-5561e8b61e7b

and reference paper :

Alday Matias, Accensi Mickael, Ardhuin Fabrice, Dodet Guillaume (2021). A global wave parameter database for geophysical applications. Part 3: Improved forcing and spectral resolution. Ocean Modelling, 166, 101848 (19p.).

https://doi.org/10.1016/j.ocemod.2021.101848

1.6.2 ARROW products

Data related to acoustic sources produced in real-time are restricted to CEA and IFREMER usage for a 6-month time span. Please contact alexis.le-pichon@cea.fr for specific data access. The product delayed by 6 months is then publicly distributed with the obligation to cite it by its DOI :

Accensi Mickael (2022). ARROW. IFREMER
https://doi.org/10.12770/76a2e647-8217-4262-99f9-284fc79d69e1

and reference paper :

De Carlo Marine (2020). Characterization of atmospheric ambiant noise originating from the ocean : global modelling of microbaroms and comparison with infrasound observations of the International Monitoring System. Oceanography. Université de Bretagne occidentale - Brest, 2020. English. NNT : 2020BRES0087. Tel-03358388 https://theses.hal.science/tel-03358388

1.7 Data and software licenses

The data production framework is based on a set of scripts and programs with restrictions of usage given below.

WAVEWATCH-III (r) : spectral wave model under LGPLv3 license, available on https://github.com/NOAA-EMC/WW3

waverun toolbox : suite of scripts designed to run WW3, under GPLv3 license, available on https://gitlab.ifremer.fr/wave/tools/waverun

Wind forcing is produced by IFS model at ECMWF, it is in restricted access for research purposes. A license must be requested on https://www.ecmwf.int/en/forecasts/accessing-forecasts

2 Product content

2.1 Overview

IFREMER delivers several products **publicly available** to the community:

- the microseism source term which contains the equivalent surface pressure spectral density, expressed in $Pa^2 \cdot m^2 \cdot s$ - proportional to the Hasselmann integral – are delivered at **quasi-real time** and has been re run as hindcast from 1993 to 2023.
  => Products : .nc files with dimensions : lat, lon, freq, time
- the acoustic sources, expressed in $W \cdot m^{-2} \cdot Hz^{-1}$ are delivered **at t+6 months**.
  => Products : .nc files with dimensions : lat, lon, freq, time

Some products are only available with **restricted access** to CEA and IFREMER :

- the acoustic sources are delivered at **quasi-real time**
  => Products : .nc files with dimensions : lat, lon, freq, time
- the acoustic transformation coefficient - transforming the equivalent surface pressure spectral density into acoustic sources.
  => Products : .nc file with dimensions: lat, lon, freq
  + code generating the coefficient
  + code applying the coefficient to the equivalent surface pressure
- the grid transformations from the lon/lat WW3 grid to the station centered grid are available for all stations.
  => Products : .nc files, one per station
  + example of the code to obtain these files
- An example of the use of these acoustic sources to generate an estimate of the density power spectrum received at the station.

The products described in this chapter are only the publicly available ones, which are the microseism source term and the acoustic sources.

The microseism source term (base ten logarithm of Hasselmann integral) at the sea surface is estimated by the spectral model WAVEWATCH-III® (WW3). It consists of the spectral density of equivalent surface pressure, expressed in $Pa^2 \cdot m^2 \cdot s$

The acoustic sources refers to the acoustic flux emitted in all vertical and azimuth directions over a square meter at z=0 in $W \cdot m^{-2} \cdot Hz^{-1}$, with only the propagative part of the flux considered. These sources are obtained by multiplying the Hasselmann integral by a

parameter, the acoustic transformation coefficient, that depends on the frequency, the depth and the elevation angles considered for the propagation and that is integrated over the elevation angles.

The grid transformation files contains addresses of the source grid (WW3 grid) that should be used to transform it into a grid centered on the station.

2.2 Product Description

2.2.1 Spatial information

The microseism source term and the acoustic sources are provided over a regular grid with a 0.5degree horizontal resolution covering the Global grid from latitudes -78° to 83° and longitudes from -180° to 179.5°.

2.2.2 Temporal information

The product outputs are available every 3 hours from 1993 to 2023 as hindcast and as real-time since 2021 January 1st.

2.2.3 Frequency content

The microseism source term is described over 22 frequencies f , exponentially increasing from 0.041019 Hz to 0.303551 Hz. The acoustic frequency equals twice the surface gravity waves frequency and therefore $f_s = 2 \times f$. For the acoustic sources, the associated f_s goes from 0.082038 Hz to 0.607102 Hz.

2.2.4 Product content

Table 1: Microseism source term product description

Parameter usual name	**Variable name**	**units**
time	time	days since 1990-01-01
longitude	longitude	degrees_east
latitude	latitude	degrees_north
wave frequency	f	s-1
base ten logarithm of power spectral density of equivalent surface pressure	p2l	log10(Pa2 m2 s+1E-12)

Table 2: Acoustic sources product description

Parameter usual name	**Variable name**	**units**
time	time	days since 1990-01-01
longitude	longitude	degrees_east
latitude	latitude	degrees_north
wave frequency	f	s-1
Acoustic frequency	fs	s-1
power spectral density of equivalent surface pressure	p2	Pa2 m2 s
acoustic power flow in the atmosphere	ap	W m-2 s

2.2.5 Computation

The microseism source term is expressed in $Pa^2 \cdot m^2 \cdot s$. It is proportional to equivalent surface pressure spectral density which is computed for each grid cell and for each frequency:

$$\rho_w^2 g^2 f_s \int_0^{\pi} E(f,\theta) E(f,\theta+\pi) d\theta$$

with ρ_w the water density, g the acceleration of gravity, f the gravity waves frequency, f_s the acoustic and seismic frequency ($f_s = 2f$) and $E(f,\theta)$ the directional wave spectrum.

The integrated acoustic flux over elevation angles and azimuth writes (based on eq.50 and on the notations in De Carlo et al. 2020):

$$ap(f_s) = \underbrace{\int_{\theta_a=0}^{\pi/2} \int_{\phi_2=0}^{2\pi} 4\pi^2 f_s^2 \cos(\theta_a)^2 \sin(\theta_a) \frac{\rho_a}{\alpha_a^3 \rho_w^2} |R_a|^2 \, d\phi_2 \, d\theta_a}_{FacAc} \cdot \underbrace{f_s g^2 \rho_w^2 \int_{\theta=0}^{\pi} E(f,\theta) E(f,\theta+\pi) \, d\theta}_{10^{P2L}}$$

The product stored is the *FacAc* factor in $s \cdot kg^{-1}$, computed for each grid cell (as the Ra term depends on the depth) and for each frequency.

2.2.6 File name convention

The filename convention for hindcast and realtime is respectively :

LOPS_WW3-GLOB-30M_<YYYMM>_p2l.nc
ARROW_WW3-GLOB-30M_<YYYYMMDDTHHZ>_p2l.nc

where :
<YYYYMM> is the covered monthly period expressed in the format YYYYMM
<YYYYMMDDTHHZ> is the covered hourly period expressed in the format YYYYMMDDTHHZ

The acoustic sources files have similar convention names except that 'p2l' is replaced by 'ap':
ARROW_WW3-GLOB-30M_<YYYYMMDDTHHZ>_ap.nc

2.2.7 File format

The files are stored in netCDF4 format with internal compression based on netCDF 4.7.3. The variable names are given in Tables 1 to 4.

```
dimensions:
        level = 1 ;
        longitude = 720 ;
        latitude = 323 ;
        f = 22 ;
        time = UNLIMITED ; // (1 currently)
variables:
        float longitude(longitude) ;
                longitude:units = "degree_east" ;
                longitude:long_name = "longitude" ;
                longitude:standard_name = "longitude" ;
                longitude:valid_min = -180.f ;
                longitude:valid_max = 360.f ;
                longitude:axis = "X" ;
        float latitude(latitude) ;
                latitude:units = "degree_north" ;
                latitude:long_name = "latitude" ;
                latitude:standard_name = "latitude" ;
                latitude:valid_min = -90.f ;
                latitude:valid_max = 180.f ;
                latitude:axis = "Y" ;
        float f(f) ;
                f:long_name = "wave_frequency" ;
                f:standard_name = "wave_frequency" ;
                f:units = "s-1" ;
                f:axis = "Hz" ;
        double time(time) ;
                time:long_name = "julian day (UT)" ;
                time:standard_name = "time" ;
                time:units = "days since 1990-01-01 00:00:00" ;
                time:conventions = "relative julian days with decimal part (as parts of the day )" ;
                time:axis = "T" ;
                time:calendar = "standard" ;
        short MAPSTA(latitude, longitude) ;
                MAPSTA:long_name = "status map" ;
                MAPSTA:standard_name = "status map" ;
                MAPSTA:units = "1" ;
                MAPSTA:valid_min = -32 ;
                MAPSTA:valid_max = 32 ;
        short p2l(time, f, latitude, longitude) ;
                p2l:long_name = "base ten logarithm of power spectral density of equivalent surface pressure" ;
                p2l:standard_name = "base_ten_logarithm_of_power_spectral_density_of_equivalent_surface_pressure" ;
                p2l:globwave_name = "base_ten_logarithm_of_power_spectral_density_of_equivalent_surface_pressure" ;
                p2l:units = "log10(Pa2 m2 s+1E-12)" ;
                p2l:_FillValue = -32767s ;
                p2l:scale_factor = 0.0004f ;
                p2l:add_offset = 0.f ;
                p2l:valid_min = -30000 ;
                p2l:valid_max = 30000 ;
```

Figure 2: Content of a netCDF file header

2.2.8 Metadata

The global attributes included in the netcdf files described the metadata.

```
// global attributes:
                :WAVEWATCH_III_version_number = "7.00" ;
                :WAVEWATCH_III_switches = "F90 NOGRB NC4 SCRIP SCRIPNC SHRD PR3 UQ FLX0 LN1 ST4 STAB0 NL1 BT4 DB1
 MLIM TR0 BS0 IC2 IS2 REF1 XX0 WNT2 WNX1 WCOR RWND CRT1 CRX1 TIDE TRKNC O0 O1 O2 O2a O2b O2c O3 O4 O5 O6 O7" ;
                :SIN4\ namelist\ parameter\ BETAMAX = 1.6f ;
                :title = "WAVEWATCH-III HINDCAST" ;
                :netcdf_version = "4.5.2" ;
                :product_name = "MARC_WW3-GLOB-30M_20210929T06Z_p2l.nc" ;
                :software_version = "v7.08_e756361_sf_rst/exe_datarmor_intel_Ifremer2_WCOR-NOIG" ;
                :references = "https://github.com/umr-lops/WW3" ;
                :source = "WAVEWATCH III (R)" ;
                :comment = "" ;
                :area = "Global 0.5 deg wave grid" ;
                :easting = "longitude" ;
                :northing = "latitude" ;
                :grid_projection = "n/a" ;
                :southernmost_latitude = "-78." ;
                :northernmost_latitude = "83." ;
                :latitude_resolution = "0." ;
                :westernmost_longitude = "-180." ;
                :easternmost_longitude = "180." ;
                :longitude_resolution = "0." ;
                :minimum_altitude = "-12000 m" ;
                :maximum_altitude = "9000 m" ;
                :altitude_resolution = "n/a" ;
                :field_type = "3-hourly" ;
                :institution = "CNRS-Ifremer-IRD-UBO" ;
                :institution_references = "https://www.umr-lops.fr/" ;
                :contact = "mickael.accensi@ifremer.fr" ;
                :distribution_statement = "No restrictions" ;
                :operational_status = "operational" ;
                :quality_index = "0" ;
                :creation_date = "2021-09-29T12:04:40Z" ;
                :product_version = "1.0" ;
                :history = "2021-09-29T12:04:40Z : Creation" ;
                :run_time = "2021-09-29T12:04:40Z" ;
                :grid = "GLOB-30M" ;
                :date_cycle = "2021-09-27T12:00:00Z" ;
                :forcing_wind = "wind_ecmwf_op" ;
                :forcing_ice = "ice_ncep_omb" ;
                :forcing_level = "no" ;
                :forcing_current = "no" ;
                :forcing_ice1 = "no" ;
                :forcing_ice2 = "no" ;
                :forcing_ice3 = "no" ;
                :forcing_ice4 = "no" ;
                :forcing_ice5 = "no" ;
                :BETAMAX = "1.60" ;
                :SWELLF = "0.66" ;
                :TAUWSHELTER = "0.3" ;
                :SWELLF3 = "0.022" ;
                :SWELLF4 = "115000.0" ;
                :SWELLF7 = "432000.00" ;
```

Figure 3: Content of the netCDF file global attributes

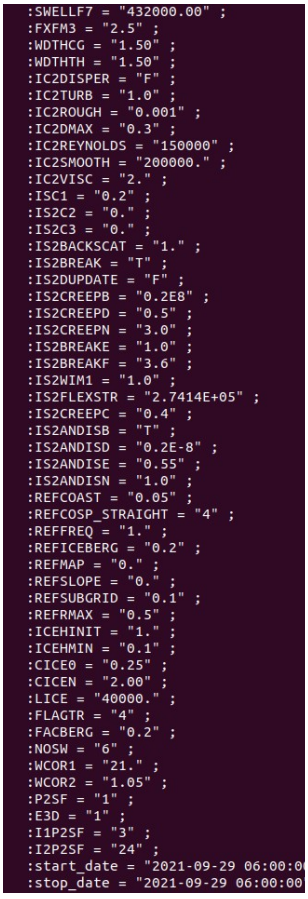

```
                :SWELLF7 = "432000.00" ;
                :FXFM3 = "2.5" ;
                :WDTHCG = "1.50" ;
                :WDTHTH = "1.50" ;
                :IC2DISPER = "F" ;
                :IC2TURB = "1.0" ;
                :IC2ROUGH = "0.001" ;
                :IC2DMAX = "0.3" ;
                :IC2REYNOLDS = "150000" ;
                :IC2SMOOTH = "200000." ;
                :IC2VISC = "2." ;
                :ISC1 = "0.2" ;
                :IS2C2 = "0." ;
                :IS2C3 = "0." ;
                :IS2BACKSCAT = "1." ;
                :IS2BREAK = "T" ;
                :IS2DUPDATE = "F" ;
                :IS2CREEPB = "0.2E8" ;
                :IS2CREEPD = "0.5" ;
                :IS2CREEPN = "3.0" ;
                :IS2BREAKE = "1.0" ;
                :IS2BREAKF = "3.6" ;
                :IS2WIM1 = "1.0" ;
                :IS2FLEXSTR = "2.7414E+05" ;
                :IS2CREEPC = "0.4" ;
                :IS2ANDISB = "T" ;
                :IS2ANDISD = "0.2E-8" ;
                :IS2ANDISE = "0.55" ;
                :IS2ANDISN = "1.0" ;
                :REFCOAST = "0.05" ;
                :REFCOSP_STRAIGHT = "4" ;
                :REFFREQ = "1." ;
                :REFICEBERG = "0.2" ;
                :REFMAP = "0." ;
                :REFSLOPE = "0." ;
                :REFSUBGRID = "0.1" ;
                :REFRMAX = "0.5" ;
                :ICEHINIT = "1." ;
                :ICEHMIN = "0.1" ;
                :CICE0 = "0.25" ;
                :CICEN = "2.00" ;
                :LICE = "40000." ;
                :FLAGTR = "4" ;
                :FACBERG = "0.2" ;
                :NOSW = "6" ;
                :WCOR1 = "21." ;
                :WCOR2 = "1.05" ;
                :P2SF = "1" ;
                :E3D = "1" ;
                :I1P2SF = "3" ;
                :I2P2SF = "24" ;
                :start_date = "2021-09-29 06:00:0
                :stop_date = "2021-09-29 06:00:00
```

Figure 4: Content of the netCDF file global attributes

3 Data Production

3.1 Overview

The data is produced in a 31-years hindcast and also as quasi real time production every 12 hours (with a 6-months delay for public access). Even if the model parameterization remains the same for those two data productions, because of real time constraints, the forcing fields for the quasi real time are not the same as for the hindcast.

WW3 model performance has been validated through an intensive process described in Alday et al. 2021 by comparing model outputs against altimeter from CCI SEA STATE database and in situ data from INSTAC and CDIP.

3.2 Hindcast Production

3.2.1 Model configuration

For the hindcast, from 1993 to 2023, the wave model was forced by winds from ERA-5 reanalysis and water velocities from CMEMS-Globcurrent. Ice concentration is taken from Ifremer SSMI-derived daily product and partial blocking of waves by icebergs distribution database from Altiberg.

Even if it is beyond the scope of this project, in addition to the global grid at 30 arc minutes (½ degree), some sub-grids have been processed to obtain model outputs with a higher spatial resolution about 10 arc minutes (1/6 degree) in East Pacific (PACE-10M), North-West Atlantic (ATNW-10M), North-East Atlantic (ATNE-10M), around Africa (Africa-10M) and spatial resolution about 3 arc minutes (1/20 degree) in Caribbean Sea (CRB-3M) and New Caledonia (NC-3M). Arctic sea over a 12 kilometers curvilinear grid was also processed.

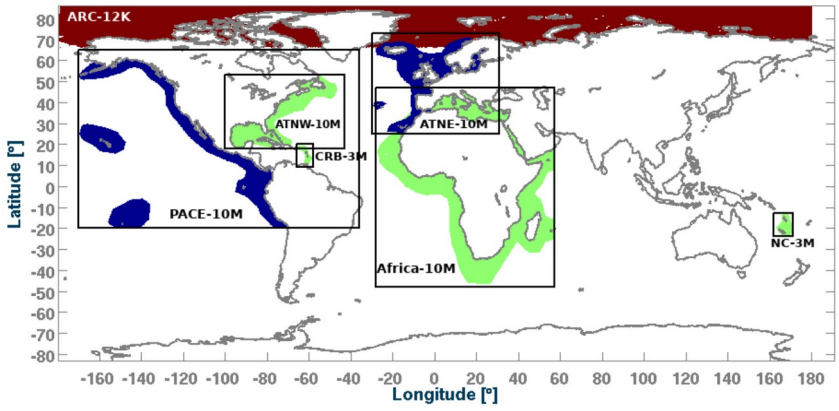

Figure 5: Map of model sub-grids domains

The 28-years hindcast used around 550,000 cpu hours distributed over 504 processors, distributed in 18 nodes that each hold 28 CPUs and 75Gb of memory. Which represents 23 hours to compute one year on the HPC.

3.2.2 Model validation

An intense validation was performed to assess the quality of the wave hindcast by comparing model outputs against altimeter and in situ data.

Many statistical parameters were used to evaluate the model-satellite discrepancy, here we only show the normalized mean difference (NMD) which is defined as follows,

$$\mathrm{NMD}(X) = \frac{\sum(X_{\mathrm{mod}} - X_{\mathrm{obs}})}{\sum X_{\mathrm{obs}}}$$

By averaging the significant wave height (Hs) over a year and comparing it against the altimeters measurements provided by the CCI SEA STATE database, we can highlight some under and overestimation of the model outputs. Even though the average bias is closed to 0, there is a positive bias in Southern Ocean and negative bias in areas with islands or coastal areas. Those discrepancies can be due to both altimeters' errors, model parameterization and wind forcing field.

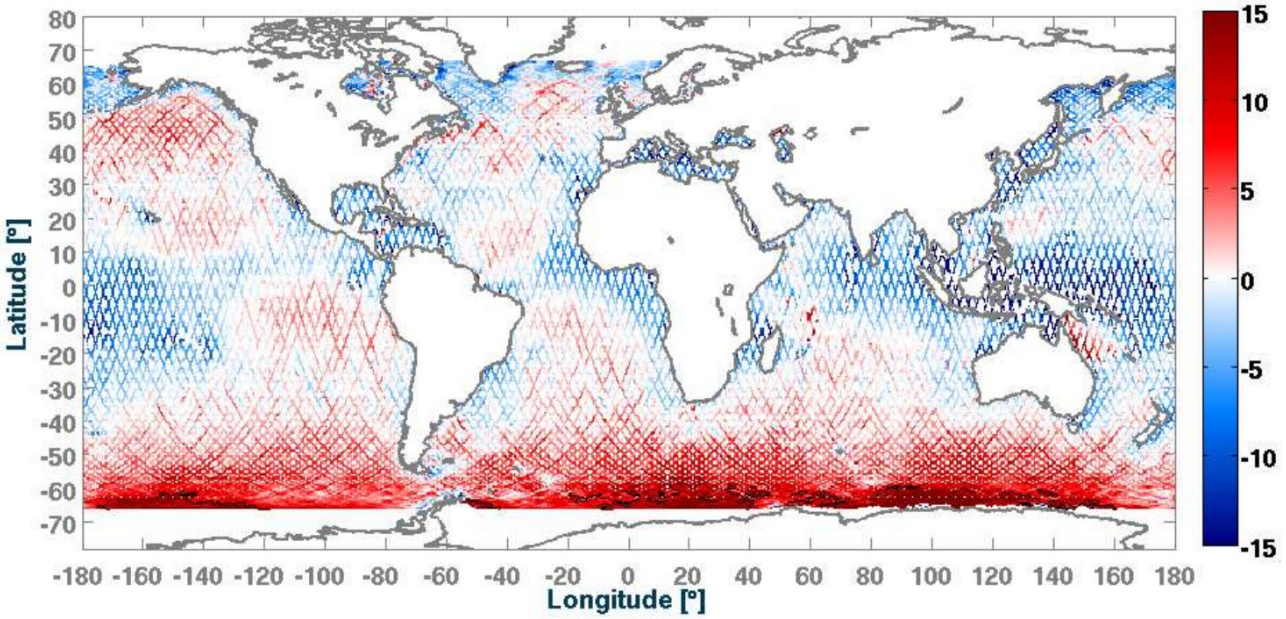

Figure 6: NMB [%] for 1-year averaged Hs for year 2011

To assess the error of wave spectra from the model output, we have selected a list of 5 relevant buoys which represent different wave climates due to their respective location, depth and distance to the coast. Because of the diameter of the buoys, we only focus on the 0.05Hz to 0.4Hz frequency band, with buoy spectra averaged over 3h intervals to be comparable to model outputs.

WMO code	latitude	longitude	depth	shore distance	buoy type
46246	50.0N	145.2 W	4252 m	900 km	Datawell WR
51208	22.285 N	159.574 W	200 m	5 km	Datawell WR
51004	17.53 N	152.25 W	5183 m	300 km	3-m discus
42097	25.7 N	83.65 W	81 m	130 km	Datawell WR
44098	42.8 N	70.17 W	77 m	37 km	Datawell WR

Figure 7: List of buoys selected for detailed validation over 2018 and 2019

The figure 8 shows different validations of the spectral content of the wave spectrum. Figures 8.(a) (left column) reveal a general good behavior of the model compared to buoy measurements with mean differences under 10% in the frequency range of interest. The deviation at high frequencies could be due to the buoys mooring line effects. At low frequencies, it may be due to the buoy heave resonance.

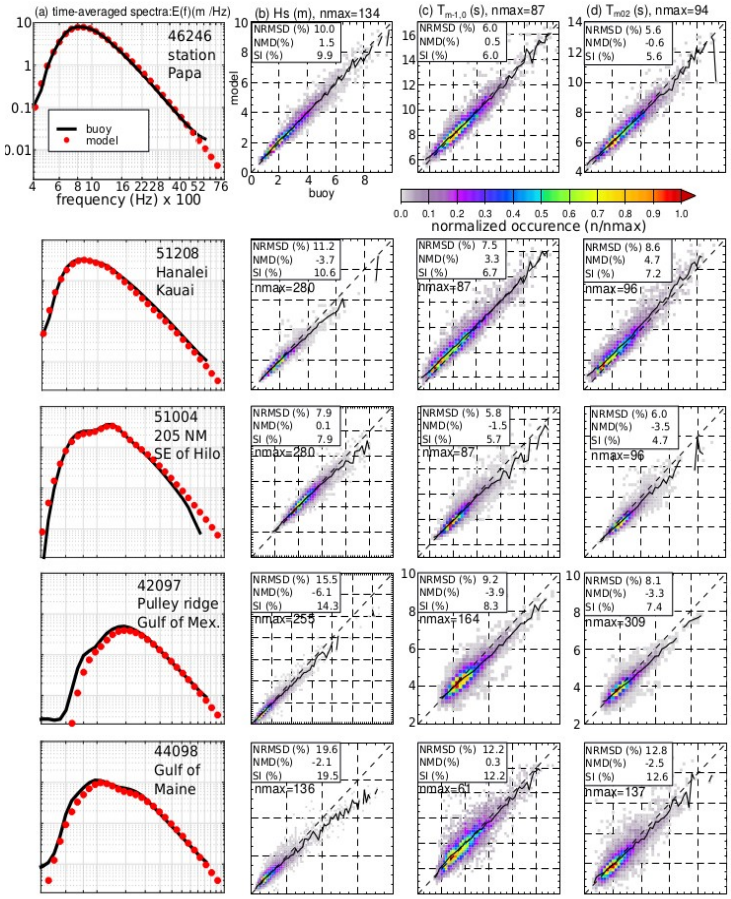

Figure 8: Modeled and measured mean spectra, scatter plots for Hs , and mean periods Tm−1,0 , Tm0,2 at selected buoys

The variability of the energy content at different frequencies is generally well captured by the parameters of significant wave height Hs (Figures 8.(b)) and mean periods Tm0,2 (which is more sensitive to the high frequencies – Figures 8.(c)) and Tm-1,0 (more sensitive to the low frequencies – Figure 8.(d)).

3.2.3 Data access

NetCDF files containing the microseism source term represent 1.3Gb per monthly file for the Global grid. The total volume of data for P2L hindcast is about 480Gb.

The description of the hindcast is available on the laboratory wave database catalog :

https://www.umr-lops.fr/Donnees/Vagues/sextant#/metadata/857a3337-f59a-481a-bf98-5561e8b61e7b

The database is available through ftp at following address :

ftp://ftp.ifremer.fr/ifremer/dataref/ww3/GLOBMULTI_ERA5_GLOBCUR_01/GLOB-30M/2020/FIELD_NC

where <YYYY> is the year between 1993 and 2023

The hindcast dataset must be cited with the following reference :

Accensi Mickael (2020). GLOBMULTI_ERA5_GLOBCUR_01. IFREMER.

https://doi.org/10.12770/857a3337-f59a-481a-bf98-5561e8b61e7b

3.3 Quasi Real-time Production

3.3.1 Model configuration

The real-time production for the 2 last days runs twice a day, at 00UTC and 12UTC. The wave model is forced by IFS winds from ECMWF and ice concentration from MERCATOR forecast product GLOBAL_ANALYSIS_FORECAST_PHY_001_024.

The 2-days hindcast used around 10 cpu hours distributed over 252 processors, distributed in 9 nodes that each hold 28 CPUs and 75Gb of memory. Which represents 2 minutes to compute 2 days.

Attention must be paid that, at the present time, no automatic validation is performed on this production. This point could be assigned for a future evolution.

3.3.2 Data access

NetCDF files containing the microseism source term represent 6Mb per hourly file for the Global grid.

Data is available as a best-estimate, which means that data is overwritten when updated by a newer prediction. For example, the run A of Day0 at 00UTC will produce data from Day-2 at 00UTC to Day0 at 00UTC. Then, the run B of Day0 at 12UTC will produce data from Day-2 at 12UTC to Day0 at 12UTC. So data of run A from Day-2 at 12UTC to Day0 at 00UTC will be overwritten by data of run B.

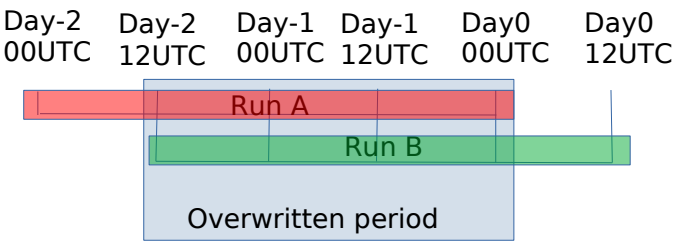

The database is available through ftp at following address :

ftp://ftp.ifremer.fr/ifremer/ww3/PROJECT/ARROW/REALTIME/ARROW/GLOB-30M/FIELD_NC/best_estimate

For validation purposes, some wave parameters (Hs, Dir, Spr, Fp, ...) are also available. Those files are referenced by the following filename convention :

ARROW_WW3-GLOB-30M_<YYYYMMDDTHHZ>.nc

where :

<YYYYMMDDTHHZ> is the covered hourly period expressed in the format YYYYMMDDTHHZ

3.3.3 Data visualization

At each time step, when a best-estimate p2l is issued, the corresponding map of microseism source term integrated over the whole frequency range is drawn as a PNG image and stored in

ftp://ftp.ifremer.fr/ifremer/ww3/PROJECT/ARROW/REALTIME/ARROW/GLOB-30M/PNG/best_estimate

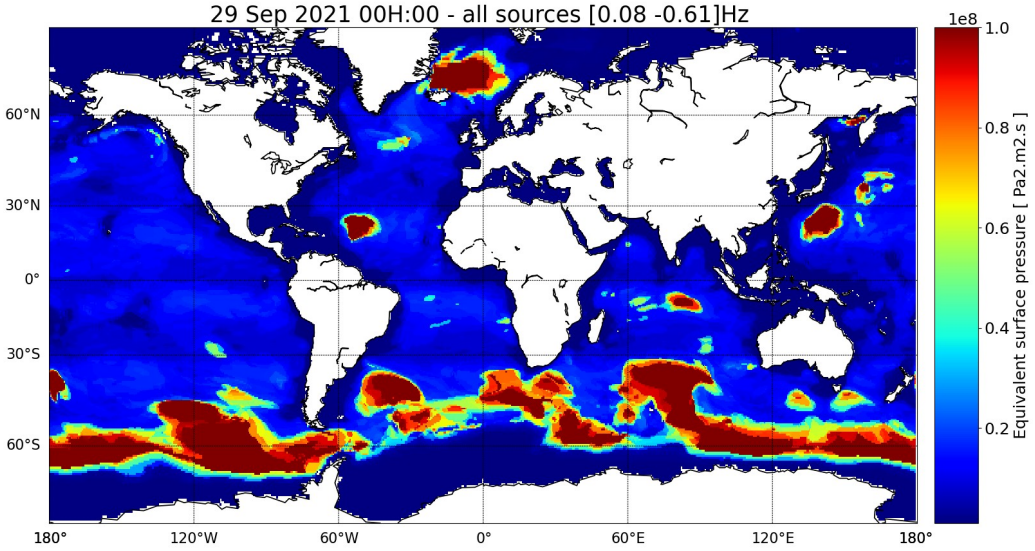

Figure 9: Map of microseism source term stored as a PNG image

The codes for the image production are available on :

ftp://ftp.ifremer.fr/ifremer/ww3/PROJECT/ARROW/TOOLS/VISU/

3.4 Acoustic Sources Processing

3.4.1 Computation

The integrated acoustic flux over elevation angles and azimuth writes (based on eq.50 and on the notations in De Carlo et al. 2020):

$$ap(f_s) = \underbrace{\int_{\theta_a=0}^{\pi/2}\int_{\phi_2=0}^{2\pi} 4\pi^2 f_s^2 \cos(\theta_a)^2 \sin(\theta_a) \frac{\rho_a}{\alpha_a^3 \rho_w^2} |R_a|^2 \, d\phi_2 \, d\theta_a}_{FacAc} \cdot \underbrace{f_s g^2 \rho_w^2 \int_{\theta=0}^{\pi} E(f,\theta) E(f,\theta+\pi) \, d\theta}_{10^{P2L}}$$

The computation of the FacAc factor requires computing an integral over the elevation angle θ_a and the azimuth ϕ_2 (resulting from the interaction) as presented in Fig. 10.a and 10.b.

As discussed in De Carlo et al. 2020, for near-vertical angles, the effect of finite depth can yield high resonance with unrealistic amplitudes (see Fig. 10.c). In order to tackle this issue in De Carlo et al. 2021 the choice was made to integrate only between 20 and 90°, thus avoiding the critical zone. Here, we wanted to be as thorough as possible, therefore accounting also for the angles between 0 and 20°.

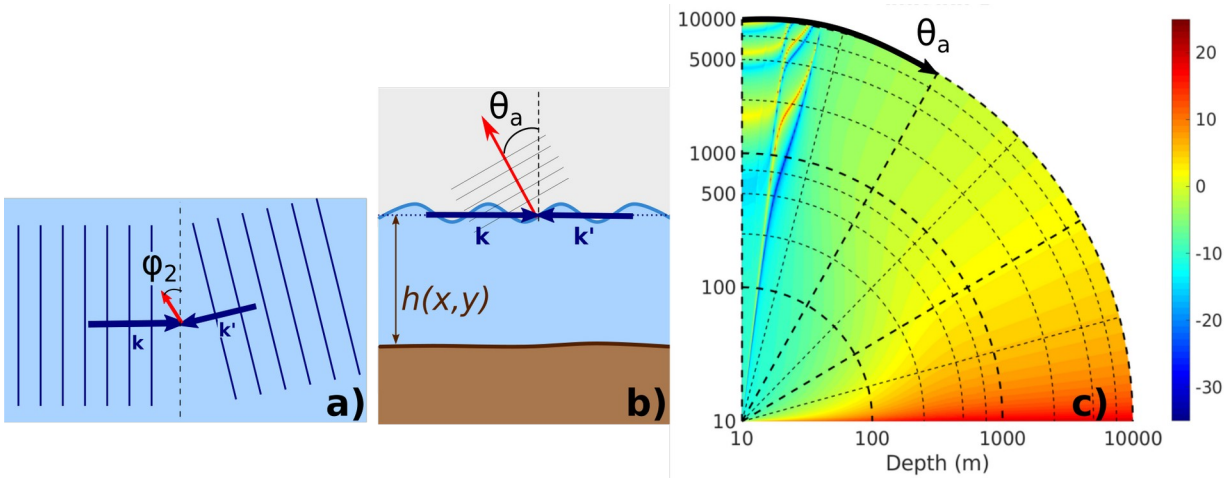

Figure 10: Wave interaction and notations: a) from above and b) from the side. c) Value of RA as presented in De Carlo et al. 2020

One way to dampen the effect of this resonance has been used in previous works (Ardhuin & Herbers, 2013, Stutzmann et al. 2012) through the addition of energy dissipation by replacing Ω by $\Omega(1-i/(2Q_R))$. As per the study, the coefficient Q_R has been chosen equal to 100 in order to stay in the acceptable seismic range and to avoid most of the resonance effects.

To further ensure that no "spike" artifact is encountered due to the sampling in θ_a, the final computation of FacAc was performed as follows:

1. For each lat/lon, freq, and ϕ_2 , the integral is computed 500 times, using $Q_R=100$, with the number of θ_a samples varying from 4500 to 5000.
2. The median of these integrated values is taken as the value for the integral for lat/lon, freq, and ϕ_2
3. These values are integrated over ϕ_2
4. FacAc is saved in a netCDF file

For each real-time time step, apart from the P2L file, a second file is created, containing p2 $p2=10^{p2l}$ and ap , which is the result of the multiplication between $p2$ and $FacAc$. This multiplication is done in command line, using the nco operators.

3.4.2 Data Access

The PNG images of acoustic power flow (see Fig. 11) are available with the 6 months delay at :

ftp://ftp.ifremer.fr/ifremer/ww3/PROJECT/ARROW/REALTIME/public/PNG/best_estimate

The netCDF files, after 6 months, are available at :

ftp://ftp.ifremer.fr/ifremer/ww3/PROJECT/ARROW/REALTIME/public/FIELD_NC/best_estimate

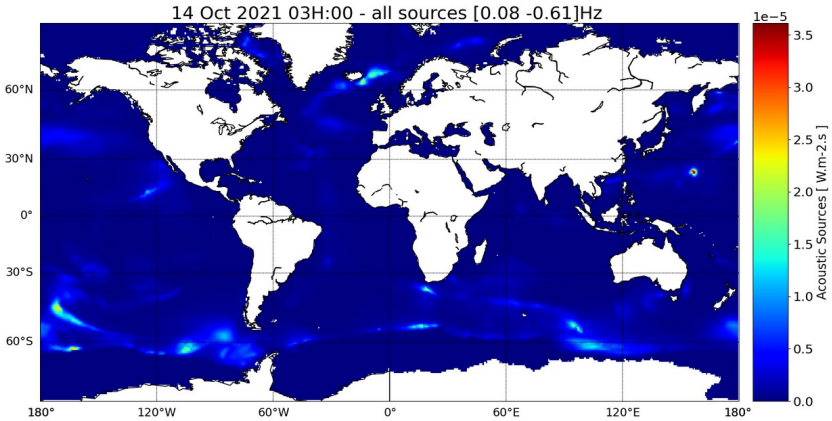

Figure 11: Acoustic sources integrated over all frequencies, for best estimate. Oct 14th 2021 3h00 UTC.